bullwinkle and *shark* regulate dorsal-appendage morphogenesis in *Drosophila* oogenesis

David H. Tran and Celeste A. Berg*

Department of Genome Sciences, University of Washington, Box 357730, Seattle, WA 98195-7730, USA
*Author for correspondence (e-mail: berg@gs.washington.edu)

Accepted 10 September 2003

Development 130, 6273-6282
Published by The Company of Biologists 2003
doi:10.1242/dev.00854

Summary

***bullwinkle* (*bwk*) regulates embryonic anteroposterior patterning and, through a novel germline-to-soma signal, morphogenesis of the eggshell dorsal appendages. We screened for dominant modifiers of the bullwinkle moose-antler eggshell phenotype and identified *shark*, which encodes an SH2-domain, ankyrin-repeat tyrosine kinase. At the onset of dorsal-appendage formation, *shark* is expressed in a punctate pattern in the squamous stretch cells overlying the nurse cells. Confocal microscopy with cell-type-specific markers demonstrates that the stretch cells act as a substrate for the migrating dorsal-appendage-forming cells and extend cellular projections towards them. Mosaic analyses reveal that *shark* is required in follicle cells for cell migration and chorion deposition. Proper *shark* RNA expression in the stretch cells requires *bwk* activity, while restoration of *shark* expression in the stretch cells suppresses the bwk dorsal-appendage phenotype. These results suggest that *shark* plays an important downstream role in the *bwk*-signaling pathway. Candidate testing implicates *Src42A* in a similar role, suggesting conservation with a vertebrate signaling pathway involving non-receptor tyrosine kinases.**

Key words: Oogenesis, Morphogenesis, *bullwinkle*, *shark*, Eggshell, Signaling

Introduction

The folding and remodeling of epithelia into more complex structures is a recurrent phenomenon in metazoan development. Intercellular interactions are important regulatory components of these processes. Adjacent cells typically provide cues that direct morphogenesis or establish an extracellular milieu permissive for cell movements.

In *Drosophila melanogaster*, remodeling epithelia can interact with an adjacent epithelium. Two well-studied examples include the migration of the embryonic dorsal epithelium over the amnioserosa (reviewed by Jacinto et al., 2002; Knust, 1997), and eversion of leg and wing primordia relative to the peripodial tissue that bounds the imaginal discs (reviewed by Fristrom, 1993). These cell layers actively regulate the patterning and movements of neighboring epithelia. Ablation of the peripodial membrane results in growth and patterning defects in the eye and wing discs (Gibson and Schubiger, 2000). In the embryo, the amnioserosa contributes signals (Harden et al., 2002; Reed et al., 2001; Stronach and Perrimon, 2001) and mechanical force (Kiehart et al., 2000) to dorsal closure. During germband retraction, the amnioserosa also signals to (Lamka and Lipshitz, 1999) and extends lamellipodia-like structures towards (Schock and Perrimon, 2002) the retracting germband cells. We elaborate on a novel extracellular pathway defined by *bullwinkle* (*bwk*) (Rittenhouse and Berg, 1995) that is essential for proper tubulogenesis of the follicular epithelium during synthesis of the dorsal appendages (DAs), specialized respiratory structures of the eggshell. Additionally, we demonstrate that an adjacent squamous cell layer acts as a substrate for the migrating epithelium and expresses factors required for this morphogenetic process.

DA formation occurs within the context of the *Drosophila* egg chamber, which consists of ~650 somatically derived follicle cells (Margolis and Spradling, 1995) surrounding a germline cyst composed of one oocyte and 15 nurse cells (Spradling, 1993). The germ cells are interconnected via cytoplasmic bridges called ring canals, which provide access for the transfer of nurse-cell material into the developing oocyte. At stage 11, the nurse cells transport most of their cytoplasm into the oocyte, and then undergo programmed cell-death (Mahajan-Miklos and Cooley, 1994). DA morphogenesis begins at stage 11, coincident with nurse-cell apoptosis.

During DA formation, the somatic layer consists of two major populations with distinctive morphologies, the stretch cells and columnar cells. At the anterior, ~50 squamous stretch cells cover the nurse cells. These cells provide signals that pattern the anterior eggshell-forming cells and ensure proper nurse-cell cytoplasmic dumping. The columnar cells overlie the oocyte at the posterior and secrete the layers and specialized structures of the eggshell (reviewed by Waring, 2000). The anterior-most columnar cells (the centripetal cells) migrate inwards, closing off the anterior end of the oocyte while synthesizing the operculum and micropyle. In addition, two subpopulations of ~65 dorsoanterior follicle cells form the two dorsal appendages through a complex reshaping and reorganization of a flat epithelium into three-dimensional tubes (Dorman et al., 2004).

These DA-forming cells apically constrict and evert outwards, changing from a flat layer into tubular structures that

extend anteriorly. Secretion of chorion proteins into the tube lumens creates the appendages (Fig. 1A). This process occurs during the final stages of oogenesis, downstream of the events that pattern the eggshell and embryonic axes.

Although much is known about the induction and refinement of follicle-cell patterning (Peri and Roth, 2000; Schüpbach, 1987; Twombly et al., 1996; Wasserman and Freeman, 1998), little is known about the factors that govern the cellular movements. One pathway that contributes to the morphogenesis is the Jun-kinase (JNK) pathway. The *Drosophila* Jun and Fos transcription factors are expressed highly in the stretch cells and in an anterior subset of the two DA-forming cell populations. Loss of JNK-pathway function results in two short paddleless DAs and defective nurse-cell cytoplasmic transport (Dequier et al., 2001; Dobens et al., 2001; Suzanne et al., 2001).

The DA-forming cells require additional extracellular cues for normal tubulogenesis. Mosaic analyses demonstrate that *bwk* is required in the germline to regulate formation of the dorsal appendages (Rittenhouse and Berg, 1995). *bwk* encodes several SOX/TCF transcription factors with pleiotropic functions (C.A.B., M. Terayama, D. H. Tran and K. Rittenhouse, unpublished), regulating dorsal follicle-cell migration, anteroposterior (AP) patterning in the embryo, and transport of nurse-cell cytoplasm into the oocyte. In *bwk* mutants, the DA-forming cells not only fail to migrate anteriorly, but instead extend much more laterally (Dorman et al., 2004), as indicated by the wide DA paddle (Fig. 1B).

To elucidate the role of *bwk* in DA formation, we set out to identify other components of this germline-to-soma signaling pathway. We screened second-chromosome deficiencies for regions that genetically interact with *bwk*. Tests of candidate mutations identified *shark* as a strong *Enhancer of bwk*. *shark* encodes an SH2-ankyrin-repeat, tyrosine-kinase protein (Ferrante et al., 1995) that functions upstream of the JNK pathway during dorsal closure of the embryo (Fernandez et al., 2000).

We show here that *shark* acts downstream of *bwk* in the squamous stretch cells and mediates the regulation of DA formation by *bwk*. Furthermore, detailed cellular analyses with stretch-cell markers show that the stretch cells provide a substrate for the DA-forming cells and appear morphogenetically active.

Materials and methods

Stocks

We used Canton S as the wild-type strain. We employed the following mutant *Drosophila melanogaster* stocks: bwk^{151} and bwk^{8482} *P*-element insertions; bwk^{CT}, an EMS mutation (C. Trent and C.A.B., unpublished); bwk^{R4}, an imprecise excision of the *8482* insertion (Rittenhouse and Berg, 1995); $shark^{1}$, an EMS mutation causing a premature stop in the second ankyrin repeat, and *UAS-Shark*$^{+}$ (Fernandez et al., 2000); $shark^{2}$ (an unmapped lethal allele, gift from Rahul Warrior); dpp^{10638} (Twombly et al., 1996); *UAS-bsk*$^{+}$ (Boutros et al., 1998); *FRT(42B) Ubi-GFP* (kindly provided by S. Luschnig and C. Nüsslein-Volhard); *Bic-C*^{AA4} and *Bic-C*^{YC33} (Mahone et al., 1995); *Bic-C*^{WC45} (Schüpbach and Wieschaus, 1991); $GAL4^{GR1}$, *UAS-FLP (*kindly provided by T. Schüpbach); $GAL4^{c415}$ (Gustafson and Boulianne, 1996); $GAL4^{A90}$ (Manseau et al., 1997); $GAL4^{55B}$ (Brand and Perrimon, 1994); and $GAL4^{T155}$ and $GAL4^{CY2}$ (Queenan et al., 1997).

The Bloomington stock center provided the second-chromosome deficiency kit, bsk^{1} and bsk^{J27}, *UAS-Src42.CA* (Tateno et al., 2000), and *FRT 42B tubP-GAL80* (Lee et al., 2000).

Deficiency screen

Second-chromosome deficiency stocks were crossed individually to *bwk* strains in an F2 screen for dominant modifiers of the bwk DA phenotype. Ten deficiency-bearing females were compared with ten siblings lacking the deficiency in two *bwk* transheterozygous backgrounds, bwk^{151}/bwk^{8482} and bwk^{151}/bwk^{CT}. Eggshell phenotypes were counted daily for 3 days, without knowing the genotype until the end of the counts.

We developed a numerical scoring system to facilitate identification of dominant modifiers. The *bwk* mutants used in the screen produced a range of phenotypes, which we sorted into four categories: wild type, short thin, short broad and very short broad. Using a weighted average in which wild type=4, short thin=3, short broad=2 and very short broad=1, we derived a score from 4 to 1 as a composite of the phenotypic classes. Eggs from $bwk^{151/8482}$ females averaged a score of 1.43, while eggs from $bwk^{151/CT}$ females averaged 2.96. The standard deviation for both allelic combinations was ~0.3. We scored eggs produced by *Df*/+; *bwk*/*bwk* females and compared these values to *bwk*/*bwk* siblings without the *Df*. Scores that differed by more than one standard deviation (0.3) were considered evidence of a significant interaction, while differences greater than 0.6 suggested strong interactions.

In situ hybridization

We subcloned the Bgl_{II} insert from a *pCaSpeR-hs-shark* plasmid (Fernandez et al., 2000) into *pBluescript-SK* and made digoxigenin-labeled RNA probes using the Roche DIG-labeling kit. We followed a modified in situ protocol (Tautz and Pfeifle, 1989; Wasserman and Freeman, 1998).

Immunofluorescence

We used the following primary antibodies: polyclonal rabbit anti-GFP (Clonetech) and monoclonal mouse anti-GFP (Molecular Probes) both at 1/100; rat anti-Fos (Riese et al., 1997) and rabbit anti-c-Jun (Chen et al., 2002) both at 1/100; mouse monoclonal anti-β-gal (Sigma) at 1/500. To detect the primary antibodies we employed secondary antibodies conjugated to Alexafluor488 and Alexafluor568 at 1/500 (Molecular Probes). We followed a modified immunocytochemistry protocol (French et al., 2003).

Mosaic analyses

Clones were induced using the FLP/FRT method (Chou and Perrimon, 1992; Xu and Rubin, 1993). Heat-shock-driven FLP produced both germline and follicle-cell clones (Golic and Lindquist, 1989). $GAL4^{GR1}$ (a gift from Trudi Schüpbach), expressed in follicle-cell stem cells and later-stage egg chambers, was used to induce follicle-cell clones. *Ubiquitin-GFP* was used to mark the clones (Davis et al., 1995).

Positively marked clones were made with a modification of the MARCM method (Lee et al., 2000). Females of genotype *hsFLP*/+; *FRT* $shark^{1}$/*FRT tubP-GAL80*; *UAS-GFP*^{S65T}/$GAL4^{T155}$ were heat-shocked for 2 hours, dissected 3-4 days post-heat-shock, and stained with anti-GFP.

Transgenic expression in bwk

UAS-shark^{+}, *UAS-bsk*$^{+}$ and *UAS-Src42A.CA*$^{+}$ were expressed using $GAL4^{c415}$, $GAL4^{55B}$ or $GAL4^{CY2}$ in a $bwk^{151/8482}$ background. Eggs laid by 10 females per genotype were examined over 3 days on egg plates. Control sibling flies lacking the GAL4 or UAS elements were also tested.

Results

Deficiency interaction screen

To identify components of the *bwk* germline-to-soma signaling

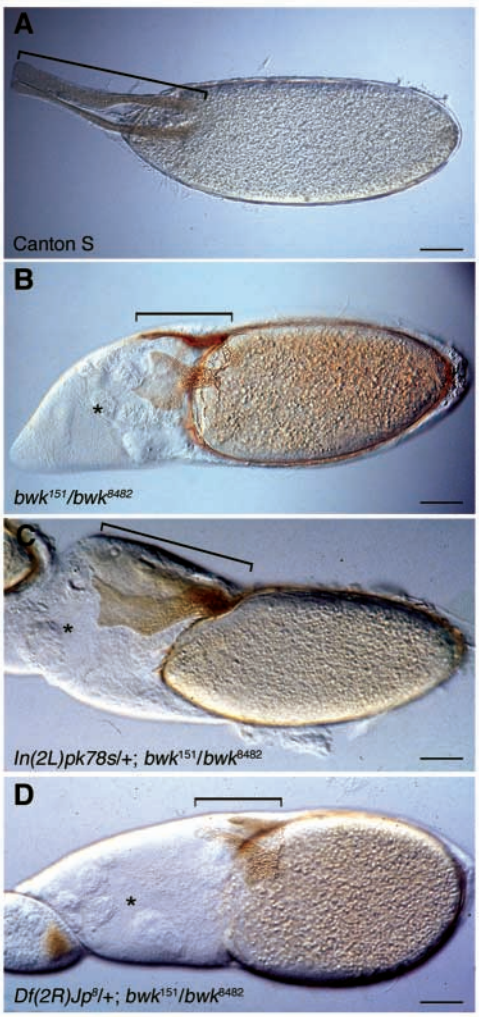

Fig. 1. Deficiencies significantly modified the bwk DA phenotype. DIC images of stage-14 egg chambers. (A) Canton S egg chamber exhibiting two long, tubular DAs (bracket). (B) bwk^{151}/bwk^{8482} egg chamber with shortened and broadened DAs (bracket). Note the remnant nurse-cell material caused by a defect in nurse-cell-cytoplasmic transport (asterisk). (C) *In(2L)pk78s*/+; $bwk^{151/8482}$ egg chamber exhibiting suppression of the DA defect. The amount of remnant nurse-cell material is unchanged (asterisk). (D) *Df(2R)Jp8*/+; $bwk^{151/8482}$ egg chamber showing an enhanced bwk DA defect. The DA length is reduced and the shape of the appendage is altered. This deletion uncovers the gene *shark*. Scale bars: 100 μm.

Table 1. Deficiencies screened for interaction with *bwk*

Deficiency	Deficiency breakpoints	Interaction
Df(2L)PMF	21A1; 21B7-8	S
Df(2L)al, cn	21B8-C1; 21C8-D1	E
Df(2L)S2	21C6-D1; 22A6-B1	E
Df(2L)ast2	21D1-2; 22B2-3	E
Df(2L)edl, al b	24A3-A4; 24D3-D4	E
Df(2L)sc19-8	24C2-8; 25C8-9	S
Df(2L)cl-h3	25D2-D4; 26B2-5	0
Df(2L)GpdhA	25D7-E1; 26A8-9	0
Df(2L)J136-H52	**27C2-9; 28B3-4**	**SS**
Df(2L)spdX4,	27E; 28C	0
Df(2L)30C	29F7-30A1; 30C2-5	0
Df(2L)Pr1	32F1-3; 33F1-2	E
Df(2L)esc10, b p r	33A8-B1; 33B2-3	0
Df(2L)osp29, Adh	35B3; 35E6	E
Df(2L)r10, cn	**35D1-D2; 36A7**	**EE**
Df(2L)H20, b pr c	36A8-9; 36E1-2	0
Df(2L)TW50, cn	36E4-F1; 38A6-7, 36F+?	E
Df(2L)E55	37D2-E1; 37F5-38A1	0
Df(2L)pr76, Sco	37D; 38E	0
Df(2L)TW84	37F5-38A1; 39D3-E1	0
Df(2L)TW161, M, p	38A6-B1; 40A4-B1	0
Df(2R)M41A4	41A	S
In(2R)pk78s	**42C1-7; 43F5-8 and In. 42C; 59F5-8**	**SS**
Df(2R)cn9	42E; 44C	0
Df(2R)44CE, al d p	44C4-C5; 44E2-4	0
Df(2R)en-A	47D3; 48A5-6	0
Df(2R)en30	48A3-4; 48C6-8	0
Df(2R)vg135	49A-B; 49D-E and In. 47F4-48A	S
Df(2R)CX1, b pr	49C1-4; 50C23-D2	0
Df(2R)trix	51A1-2; 51B6	0
Df(2R)Jp1	51C3-52F5-9	E
Df(2R)Jp8, w[+]	**52F5-9; 52F10-53A1**	**EE**
Df(2R)Pc111B, al	54F6-55A1; 55C1-3	0
Df(2R)PC4	55A; 55F	0
Df(2R)AA21, In(2R)	56F9-17; 57D11-12, 38E;	S
Df(2R)PuD17, cn b	57B4; 58B	E
Df(2R)or-BR6, cn	59D5-10; 60B3-8	0
Df(2R)Px4, Dp(2L)	60B; 60D1-2	0
Df(2R)Px2	60C5-6; 60D9-10	0

Third column indicates the interaction [no interaction (0), enhancement (E) or suppression (S)] of the bwk eggshell phenotype. One E or S denotes a significant interaction (see Materials and methods), two letters (EE or SS) indicate a strong interaction.

pathway, we undertook a deficiency screen looking for dominant genetic interactions with *bwk*. We examined the effect of heterozygous deficiencies upon the DA morphology of *bwk* eggs. This approach allowed the identification of genes sensitive to levels of *bwk* activity, including those with pleiotropic functions.

We employed two allelic combinations to facilitate isolation of both enhancers and suppressors: $bwk^{151/8482}$, a strong loss-of-function combination (Fig. 1B), and $bwk^{151/CT}$, a moderate loss-of-function combination. Both combinations produced a range of phenotypes. $bwk^{151/8482}$ eggs have mainly short, broad dorsal appendages, facilitating the identification of suppressing mutations. $bwk^{151/CT}$ eggs manifest an array of DA structures from short, broad to long, tubular appendages. As $bwk^{151/CT}$ phenotypic profile exhibited a bias towards wild-type length DAs, this combination facilitated the isolation of enhancing interactions.

The Bloomington Stock Center maintains a large collection of deletions that uncover 60-70% of the *Drosophila* genome. We screened 39 deficiencies that uncover ~78% of the second chromosome, as determined by polytene-segment coverage (Table 1). We scored F_2 progeny to examine the effect of these deletions on the DA phenotypes of the two *bwk*-allele combinations. Using a stringent scoring method (see Materials and methods), we identified four deletions that exhibited a strong interaction, two enhancers and two suppressors. Nine deletions exhibited a moderate interaction and seven interacted weakly. We focused our initial efforts on the four strong modifiers.

Identification of interacting loci

The *Df(2L)J136-H52* and *In(2R)pk78s* chromosomes (Fig. 1C) strongly suppressed the bwk DA phenotype, while *Df(2L)r10 cn* and *Df(2R)Jp8* (Fig. 1D) strongly enhanced it. Extensive analyses using overlapping and smaller deficiencies failed to

recapitulate the suppression associated with both *Df(2L)J136-H52* and *In(2R)pk78s* (data not shown). Similar studies did confirm the two strong enhancing interactions and defined the interacting segments as 35D1-35E2 and 52F5-53A. Tests with available mutations in these regions indicated that heterozygous loss of function of either *Bicaudal-C* (35E2) or *shark* (52F) enhanced the bwk DA phenotype (data not shown). We focused our efforts on *shark* due to a previously reported function for this gene in regulating epithelial morphogenesis (Fernandez et al., 2000).

shark is a strong *Enhancer of bwk*

A mutation resulting in a premature stop codon in the *shark* gene (Ferrante et al., 1995) showed strong enhancement of the bwk phenotype, similar to the original deficiency (data not shown). Germline clones of *shark*^{1}, however, failed to produce a detectable phenotype in oogenesis (Fernandez et al., 2000), leading us to investigate a possible somatic function.

First, we examined expression of *shark* in oogenesis and noticed an unusual pattern (Fig. 2). *shark* transcript was present in the germline and somatic cells beginning in region 2 of the germarium (Fig. 2A). At the time of dorsal-appendage formation, egg chambers showed a pronounced pattern of discrete spots and tracks near the periphery of the nurse cells (Fig. 2C). These foci were often associated with stretch-cell nuclei (arrowheads, Fig. 2C′), suggesting that *shark* expression occurs in the thin (<1 μm) stretch-cell layer overlying the nurse cells. After stage 10, during rapid nurse-cell cytoplasmic transport, *shark* RNA levels increased dramatically in the nurse cells and the unusual foci were no longer readily visible (data not shown).

bwk mutants exhibited an altered pattern of *shark* mRNA localization (Fig. 2B,D,D′). Although germline staining resembled wild type, the discrete foci were not evident at stage 10 (compare Fig. 2C′ with 2D′). These results suggest that the *bwk* pathway normally modulates *shark* expression in the stretch cells, implicating this layer in DA formation. Previous studies, however, had not described a role for stretch cells in this process. We therefore examined the behavior and morphology of the stretch cells during DA morphogenesis.

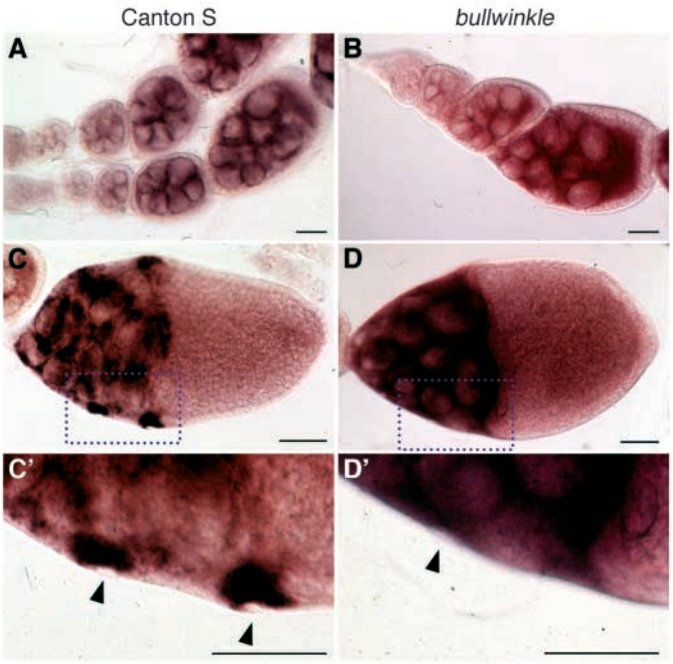

Fig. 2. *shark* expression is altered in *bwk* mutants. In situ hybridization of egg chambers probed with antisense *shark* RNA in Canton S (A,C,C′) and in *bwk*$^{151/8482}$ egg chambers (B,D,D′). (A) In early oogenesis, *shark* RNA is expressed in all tissues, with higher levels in the germline. (C) Surface view. At stage 10, *shark* RNA accumulates in darkly staining concentrations at the periphery of nurse cells. Boxed area shows RNA foci associated with stretch-cell nuclei. Faint expression in the columnar cells over the oocyte is also seen. (C′) Magnified view of the boxed area in C. Arrowheads indicate stretch cell nuclei. (B) In *bwk* egg chambers, the RNA appears more diffuse, although levels are comparable with wild type. (D) At stage 10, the concentrated RNA foci at the anterior are greatly reduced (compare with C). (D′) Magnified view of area outlined by blue box in D. Arrowhead indicates stretch cell nucleus. Scale bars: 100 μm.

Stretch cells act as a substrate for DA formation

We examined egg chambers that expressed both stretch-cell-specific and columnar-cell-specific markers. To label stretch cells, we employed the GAL4/UAS system (Brand and Perrimon, 1993), driving *UAS-GFP*^{S65T} with *GAL4*^{c415} or *GAL4*^{A90} (Gustafson and Boulianne, 1996; Manseau et al., 1997). *c415* drives reporter expression in the stretch cells while *A90* labels both the stretch cells and the border cells. To mark the DA-forming cells, we used the *P[lacZ; ry*$^{+}$*]* enhancer trap line *PZ05650*, which expresses highly in the centripetally migrating columnar cells and in the two populations of dorsoanterior follicle cells that synthesize the dorsal appendages (Rittenhouse and Berg, 1995).

At stage 10, the stretch cells covered the exterior of the nurse cells (Fig. 3A,B). The thinness of the layer meant that the cells were most visible at the junctions of nurse cells (Fig. 3A′, blue arrowhead) and in regions surrounding the nuclei of the stretch cells (Fig. 3A′, blue triangle). This morphology of the stretch cells, a significant thickening of the layer at discrete locations, could explain the *shark* RNA foci: localized cell thickening could cause ubiquitously expressed RNA to appear localized. Alternatively, the *shark* foci could represent actual localization of RNA within the stretch cells.

During centripetal migration at stage 10B, the posterior-most stretch cells also migrated inwards (asterisk, Fig. 3A) accompanying centripetally migrating columnar cells (red nuclei, Fig. 3B). These panels show two egg chambers: the follicle cells in the upper egg chamber have nearly completed centripetal migration, while those in the egg chamber on the lower right, a partial view, have just initiated this process (arrow, Fig. 3B).

At stage 12, the nurse cells were much smaller due to transport of their cytoplasm into the oocyte (compare the nurse cells, labeled NC, in Fig. 3C with those in 3A), while the stretch cell layer had thickened. At this time, the stretch cells exhibited three interesting behaviors. First, in contrast to stage 10, the stretch cells enveloped all nurse cells (Fig. 3C). This envelopment could be due to an active movement or a by-product of the nurse-cell shrinkage. Second, the migrating DA-forming cells moved over the stretch cells (green arrowhead, Fig. 3C). Finally, the stretch cells occasionally extended small cellular projections towards the DA-forming cells (arrow, Fig.

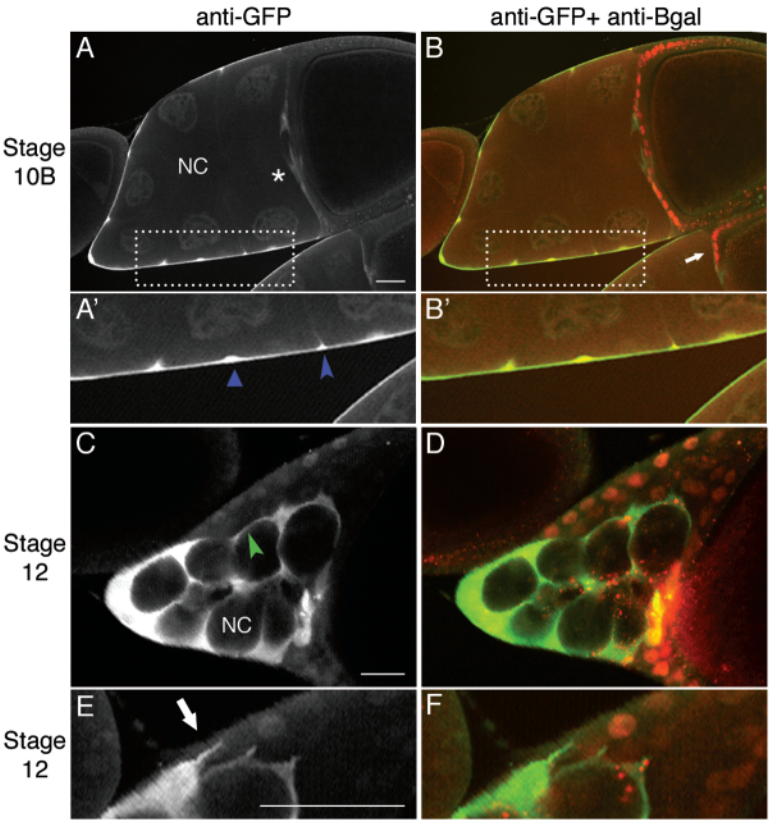

Fig. 3. Stretch cells are a substrate for DA-forming cells and exhibit morphogenetic behaviors. Confocal images of Canton-S egg chambers expressing *UAS-GFP*^{S65T} in the stretch cells and a nuclear β-galactosidase in the anterior columnar cells. (A,A′,C,E) Anti-GFP, (B,B′,D,F) merge of anti-GFP (green) and anti-β-gal (red) images. (A,B) The stretch cells cover the exterior of the nurse cells. The posterior-most stretch cells (asterisk in A) move inwards along with the centripetally migrating columnar cells. In the lower right of panels A and B, centripetal migration is commencing in a stage-10B egg chamber (white arrow in B). (A′,B′) Magnified views of the boxed areas in A,B show that the stretch-cell layer is thickest near the stretch-cell nuclei (blue triangle, A′) and at the valleys between nurse cells (blue arrowhead, A′). (C,D) Stretch-cell staining is present around the shrinking nurse cells (NC). The DA-forming cells have formed a tube and are moving anteriorly on the stretch cells (green arrowhead, C). (E,F) A magnified view of an interface between the front of a DA-cell wedge and the stretch cells at stage 12. Note the thin cellular projections extending towards the DA cells (arrow). Scale bars: 25 μm.

3E,F). By stage 13, the stretch cells resided between and underneath the two DA cell populations, which have reached the anterior end of the egg (data not shown).

These studies revealed that the stretch cells are a substrate for the migrating DA-forming cells. This result contradicts a previous hypothesis (King and Koch, 1963), who proposed that the DA-forming cells migrated between the stretch and nurse cells in an invasive manner. Thus, the stretch cells form an intervening layer between the germ cells and the migrating DA-forming cells. The stretch cells could express factors that mediate the movement of the DA cells across this layer; *shark* may be such a factor, as suggested by the genetic interaction and expression data. Because the known *shark* alleles are lethal, we used mosaic analyses to examine the function of *shark* in oogenesis.

shark clones exhibited DA defects in oogenesis

We induced clones with the *shark*^{1} (Fernandez et al., 2000) and *shark*^{2} (R. Warrior, unpublished) alleles using the FLP/FRT system (Xu and Rubin, 1993). We expressed FLP using either a *heat-shock promoter-FLPase* transgene or a follicle-cell-specific GAL4 transgene, *GR1*, driving *UAS-FLP*. *GAL4*^{GR1} is expressed in the follicle cells continuously from the time of stem-cell division to stage 14 (T. Schüpbach, personal communication). We marked the clonal cells in two fashions: negatively, such that loss of *Ubiquitin-GFP* (Davis et al., 1995) defined homozygous *shark* cells, or positively, with a modification of the MARCM/GAL80 method (Lee et al., 2000). In positively marked clones, only homozygous *shark* cells expressed *UAS-GFP*^{S65T} (Amrein and Axel, 1997).

shark clones affected the morphology of the dorsal appendages and the structure of the DA chorion (Fig. 4). In some eggs (Fig. 4A,E), the DA material appeared vacuolated, with gaps interposed with a skeletal network. This phenotype resembled defects seen in mutants affecting eggshell structure (reviewed by Waring, 2000). In contrast to chorion mutants, however, *shark* mosaic eggs with clones in the main body had no obvious structural defect (data not shown).

Other eggs displayed shortened DAs with normal chorion, suggesting a defect in the anterior migration of the DA-forming cells (Fig. 4B). The shortness of the dorsal appendages varied from the egg in Fig. 4B to the egg in Fig. 4C.

The chorion and short-DA defects were not mutually exclusive; in fact, most chorion-defective appendages were also shortened. These defects were associated with clones in the anterior of the egg; when the entire anterior was clonal, both DAs were short and vacuolated (data not shown).

To establish the precise relationship between clone position and DA defect, we examined small clones and their effect on DA morphology. Scoring small clones by the absence of GFP proved difficult; however, once the DA cells had migrated onto the stretch cells. We used positively marked clones for clarity. In one representative clone, most GFP-positive clonal cells lay between the two DAs (Fig. 4C-G). By position, many of these marked cells should be stretch cells. Several of the GFP-positive cells were also closely associated with the chorion-defective DA, and likely label the DA-forming cells responsible for secreting the appendage chorion in E.

The frequency of these defects was low (Fig. 4H). Clone frequency, as measured by the number of egg chambers with at least one clone, for post-mitotic stages varied from 14.2 to 17.4%. No defects were seen with a wild-type FRT chromosome, while an FRT *shark*^{2} chromosome recapitulated the *shark*^{1} results. Most clones were made with the *shark*^{1} allele, where 7.5% of all stage-14 egg chambers showed a DA chorion defect and 1.9% had short DAs with normal DA chorion. We attribute this low frequency to several factors: regional specificity within the egg chamber, large clone-size

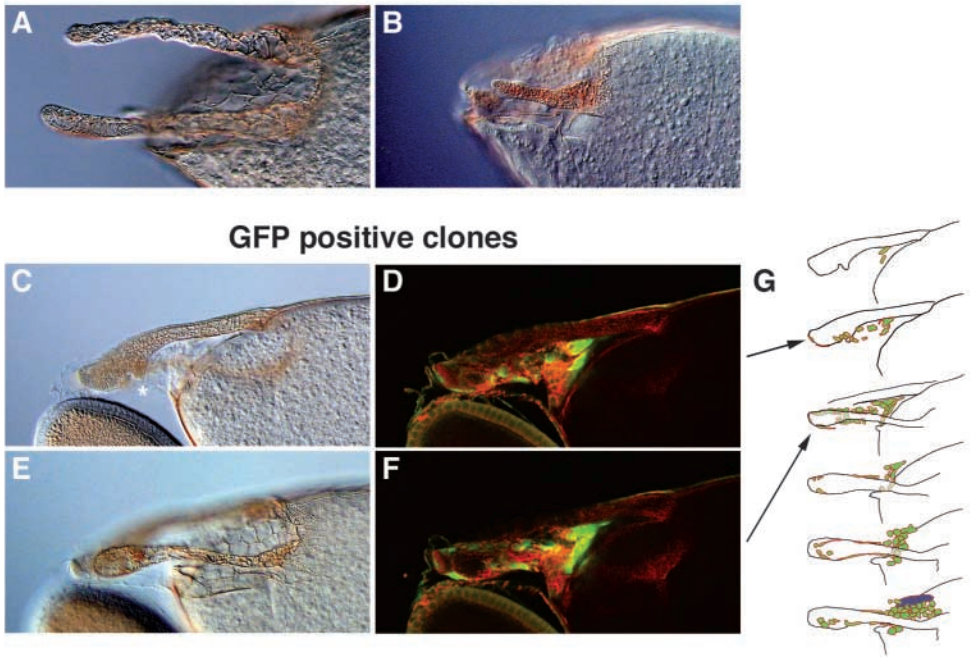

Fig. 4. *shark* follicle-cell mosaics produce two distinct DA phenotypes. (A,B) DIC images of *shark*^{1}-mosaic egg chambers. (A) DA chorion defect. (B) Short DA with normal chorion. (C-F) DIC and confocal images of a single egg chamber in which only the *shark*^{1} clonal cells are GFP positive. GFP-positive cells are green and anti-α-Spectrin in red shows cell membranes. Asterisk in C indicates abnormal 'thumb' of chorion in anterior of the right DA (C,D). The left DA (E,F) is vacuolated. (G) Diagrams of six confocal *z* slices taken 3 μm apart of egg chamber in C-F. Arrows indicate the corresponding *z* slice for the two confocal images shown. GFP-positive cells are labeled green. A region where the cell boundary is indeterminate is shown in purple. *shark*^{1} clonal cells lie between the two DA arms or are closely associated with the DA shown in E,F. (H) Table showing frequency of clones and defects.

H

Frequency of shark mosaic DA phenotypes

		Stage 14 phenotypes		
	Clone Frequency$	Wildtype DAs	DA chorion defect&	Short DAs only
FRT *shark*^{1}	16.0%	326 (90.6%)	27 (7.5%)	7(1.9%)
FRT *shark*^{2}	17.4%	18 (75.0%)	5 (20.8%)	1 (4.2%)
Control clones	14.2%	117 (100.0%)	0	0

$ frequency for post-mitotic stages
& includes DAs that are short and chorion defective.

requirement and incomplete penetrance for the short DA defect.

These studies showed that when a significant fraction of DA-cells was clonal, a chorion defect was seen. The large-clone-size requirement implied that neighboring *shark*$^{+}$ cells could provide cell non-autonomous function for the homozygous *shark* cells. This effect was limited to the appendage associated with the clone; one DA could be affected while the other was normal.

The short-DA defects were, in turn, associated with large clones encompassing the stretch cells. These short-DA defects exhibited a variety of morphologies, from short and thin to short and broad like *bwk* mutant DAs. Furthermore, the short-DA defect was not fully penetrant; large clones in the stretch cells could result in mild defects.

To determine the relative contributions of these *shark* functions in regards to *bwk*, we asked whether tissue-specific expression of a wild-type *shark*$^{+}$ transgene could ameliorate the DA defects of a *bwk* mutant. As the stretch cells do not express or secrete chorion (Margaritis et al., 1980), we could distinguish between the role of *shark* in chorion production versus DA migration.

Expression of *UAS-shark*$^{+}$ suppresses *bwk*

We postulated that *bwk* functioned to regulate *shark* expression and/or activity in the stretch cells. Restoration of *shark* expression in the stretch cells could compensate for loss of *bwk*, if *shark* expression in these cells was a key downstream factor. To test this hypothesis, we expressed *UAS-shark*$^{+}$ (Fernandez et al., 2000) in a *bwk* background using *GAL4*^{c415}, which expresses specifically in the stretch cells (Manseau et al., 1997), *GAL4*^{55B}, which expresses in both the stretch cells and DA cells (Brand and Perrimon, 1994), and *GAL4*^{CY2}, which expresses in all follicle cells (Queenan et al., 1997).

Expression of a wild-type *UAS-shark*$^{+}$ with the *c415* and *55B* drivers suppressed the *bwk*-mutant DA phenotype substantially (Fig. 5B; Table 2A), while *CY2*-driven expression had little effect (Table 2A). With stretch-cell-specific expression of *UAS-shark*, we generated a significant shift towards longer and more tubular DAs, a more wild-type-like phenotype. We quantified the suppression using a weighted average of four classes of DA phenotypes, where a difference of greater than or equal to 0.3 between the experimental and control scores indicated a significant interaction (see Materials and methods). The *c415*-driven suppression was equivalent to the strongest suppression observed in the deficiency-interaction screen. This result indicated that *shark* expression in the stretch cells is a key factor downstream of *bwk*. Additionally, the chorion function of *shark* was not crucial to the bwk DA phenotype. To explore *shark* function in the stretch cells, we assayed candidate factors that might act with *shark* in this tissue.

Testing factors expressed in stretch cells

As Shark acts in the Jun-kinase pathway during embryonic

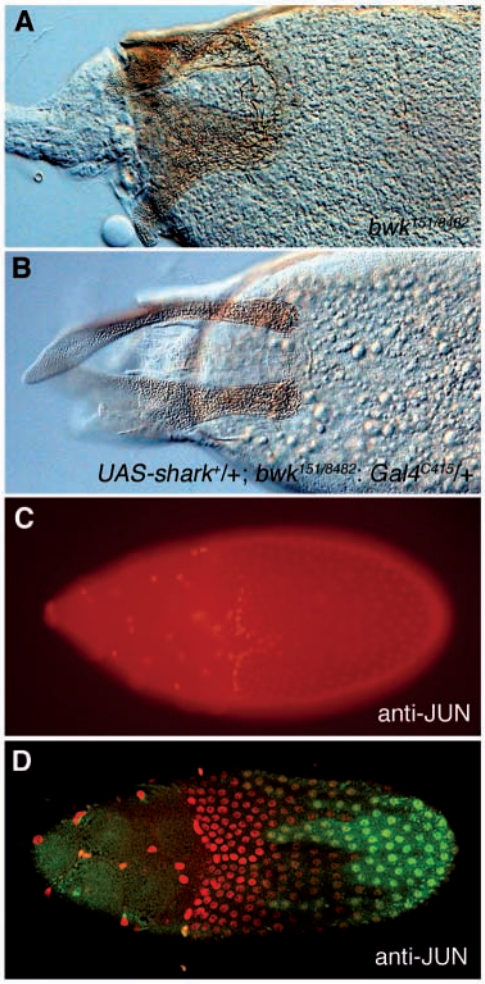

Fig. 5. *bwk*, *shark* and Jun interactions in oogenesis. (A,B) *UAS-shark*$^{+}$ suppresses the bwk$^{151/8482}$ phenotype when expressed in stretch-cells. (A) DIC image of bwk$^{151/8482}$ DA phenotype. (B) DIC image of *UAS-shark*$^{+}$ mediated suppression of bwk$^{151/8482}$ DA phenotype: DAs are longer and more tube-like. (C,D) Jun expression is unchanged in *bwk*. (C) Image of a wild-type stage-10 egg chamber showing immunofluorescence of the *Drosophila* Jun pattern in follicle cells. (D) Merged confocal image showing anti-Jun staining in a stage 10 egg chamber with a large *shark* clone (GFP-negative cells) covering most of the anterior follicle cells, including the stretch and DA-forming cells. Jun expression is unchanged.

dorsal closure (Fernandez et al., 2000) and JNK-pathway function is required for DA morphogenesis (Dequier et al., 2001; Dobens et al., 2001; Suzanne et al., 2001), we asked whether the Jun-kinase pathway is a component of the *bwk/shark* pathway in oogenesis. We tested whether gain or loss of Jun kinase (*basket*) affected bwk phenotypes (Table 2B). Basket activates both Jun and Fos in *Drosophila* (Ciapponi et al., 2001; Riesgo-Escovar et al., 1996).

Expression of *UAS-bsk*$^{+}$ led to a reduction in the number of eggs laid by *bwk* mothers but the morphology of the *bwk* DAs was not modified. Heterozygosity for two strong loss-of-function alleles (*basket*^{1} and *basket*^{J27}) also failed to interact with *bwk* (Table 2B). Additionally, expression and localization of both Jun and Fos were normal in *bwk* mutants or *shark* clones (Jun, Fig. 5C,D; Fos, J. Dorman and C.A.B., unpublished).

Another likely candidate gene expressed in the stretch cells is *dpp*, partial overexpression of which can result in shortened and fringed DAs (Twombly et al., 1996). Expression of both *dpp* RNA and a *dpp-lacZ* enhancer trap were normal in *bwk* mutants (data not shown). Heterozygosity of *dpp* and/or its receptor failed to modify the strong *bwk*$^{151/8482}$ combination (Table 2C), although modest interactions occurred with the moderate *bwk*$^{151/CT}$ combination (data not shown).

In mammalian cells, proteins related to Shark act alongside Src kinases in mediating immunoreceptor signaling (Latour and Veillette, 2001). We tested the *Drosophila Src42A* gene for interaction with *bwk*. *Src42A*, like *shark*, functions upstream of the JNK pathway in dorsal closure (Tateno et al., 2000). Interestingly, *Src42A* mutations enhanced the moderate bwk$^{151/CT}$ DA phenotype (Table 2D). Expression of transgenic *UAS-Src42A.CA*, an activated form (Tateno et al., 2000), with the stretch-cell-specific *GAL4*^{c415} suppressed the strong bwk DA phenotype (Table 2D). Compared with the *UAS-shark* suppression, the *UAS-Src42A.CA* suppression was weaker but still produced a significant shift towards longer DAs.

Discussion

Previous analyses of *bullwinkle* revealed the existence of a germline pathway required for DA morphogenesis (Rittenhouse and Berg, 1995). We screened the second-chromosome deficiency kit for modifiers of *bwk*; follow-up studies identified two *Enhancers of bwk* encoded by the *Bic-C* and *shark* genes. Although Bwk probably acts as a transcription factor, it does not directly regulate either gene. Preliminary studies (not shown) suggest that the interaction between *Bic-C* and *bwk* is complex; here we show that *shark* acts downstream of *bwk*, mediating the signal from germline to DA-forming cells.

shark functions downstream of *bwk*

shark encodes a distinctive multidomain protein that regulates the movements of epithelial cells in the dorsal embryonic epidermis (Fernandez et al., 2000). This non-receptor kinase is conserved, with homologs in *Hydra* (Chan et al., 1994) and sponge (Suga et al., 1999). The mammalian counterparts contain homologous SH2 and tyrosine-kinase domains but lack the ankyrin repeats (Chan et al., 1991; Taniguchi et al., 1991). These mammalian proteins, Zap70 and Syk, are recruited to immunoreceptor complexes upon ligand binding and regulate immune-cell activation and differentiation, functioning alongside Src kinases (reviewed by Chu et al., 1998). In T-cells, Zap70 also mediates signaling downstream of integrin-receptor complexes that feature in T-cell motility (Bearz et al., 1999; Soede et al., 1998).

We show that *shark* has two functions in oogenesis and that a *bwk/shark* pathway could involve the Shark and Src42A kinases in an evolutionarily conserved version of the mammalian signaling pathway.

shark function is required for DA structure and DA-cell movement

Mosaic analyses with loss-of-function *shark* alleles established two somatic functions in DA formation (Fig. 6). First, *shark* is required in the DA cells for proper DA-chorion deposition, a complex process regulated at many levels (reviewed by

Table 2. Shark and Src42A gain and loss of function significantly modify the bwk phenotype

Genotype: Gal4*	Dorsal appendage phenotypes WT	ST	SB	VSB	N	Score (control score)	ΔScore
(A) *bwk* $^{151/8482}$: c415	0.0%	0.0%	10.6%	89.4%	84	1.1	
shark^{1}/+; *bwk*$^{151/8482}$	0.0%	0.0%	29.4%	70.6%	17	1.3 (1.7)	**–0.4 (E)**
UAS-shark^{+}/+; *bwk*$^{151/8482}$: c415	0.4%	22.6%	64.7%	12.3%	252	2.1 (1.1)	**+1.0 (SS)**
UAS-shark^{+}/+; *bwk*$^{151/8482}$: 55B	0.0%	1.4%	40.5%	58.1%	74	1.4 (1.1)	**+0.3 (S)**
UAS-shark^{+}/+; *bwk*$^{151/8482}$: CY2	1.1%	1.1%	14.1%	83.7%	92	1.2 (1.1)	**+0.1**
(B) *bsk*^{2}/+; *bwk*$^{151/8482}$	0.0%	0.0%	14.3%	85.7%	112	1.1(1.2)	**–0.1**
UAS-bsk^{+}/+; *bwk*$^{151/8482}$: c415	0.0%	0.0%	3.1%	96.9%	33	1.0 (1.0)	**0.0**
(C) *dpp*^{10638}/+; *bwk*$^{151/8482}$	0.0%	0.0%	27.0%	73.0%	152	1.3 (1.1)	**+0.2**
sax^{5}/+; *bwk*$^{151/8482}$	0.0%	0.0%	17.6%	82.4%	68	1.2 (1.0)	**+0.2**
tkv^{7}/+; *bwk*$^{151/8482}$	0.0%	0.0%	9.1%	90.9%	44	1.1 (1.2)	**–0.1**
(D) *bwk*$^{151/CT}$	3.0%	29.8%	62.8%	4.5%	199	2.3	
Src42^{E}/+; *bwk*$^{151/CT}$	0.0%	3.6%	88.1%	8.3%	169	2.0 (2.3)	**–0.3 (E)**
UAS-Src42A.CA/+; *bwk*$^{151/8482}$: c415	0.0%	2.4%	60.0%	37.6%	125	1.7 (1.2)	**+0.5 (S)**

WT, wildtype; ST, short, thin; SB, short, broad; VSB, very short, broad DAs.

*c415, stretch cells; 55B, stretch cells + DA cells; CY2, all follicle cells. GAL4s are heterozygous and on various chromosomes.

Percentage of each DA category and total number of eggs is listed. A change in score greater than 0.3 indicates a significant interaction (S, suppression; E, enhancement).

(A) *UAS-shark*; *bwk*$^{151/8482}$, with various GAL4 drivers, showing moderate-strong suppression of the bwk$^{151/8482}$ DA phenotype. The strongest suppression occurred with the stretch-cell *GAL4*^{c415}.

(B) *UAS-bsk*$^{+}$ and *bsk*/+ mutants fail to modify the bwk$^{151/8482}$ DA phenotype.

(C) *dpp*-pathway components also fail to significantly modify *bwk*$^{151/8482}$.

(D) A strong *Src42A* mutation strongly enhances the bwk$^{151/CT}$ DA phenotype. Conversely, *UAS-Src42A.CA* driven by *GAL4*^{c415} moderately suppresses.

Waring, 2000). Mutations that disrupt chorion-gene amplification or chorion-protein synthesis result in thin, collapsed DAs and main-body eggshell (Bauer and Waring, 1987; Landis et al., 1997; Mohler and Carroll, 1984; Nilson and Schüpbach, 1998).

Unlike those mutations, loss of *shark* in the main-body follicle cells does not cause defects in follicular imprints, alter the appearance of the eggshell under darkfield optics, or produce thin chorion and collapsed eggs. Although our methods may miss subtle defects in main-body chorion, *shark* may play a DA-cell-specific role in the production/formation of chorion. Although regulatory sequences and a putative binding protein drive specific spatial expression of chorion-reporter constructs (Tolias and Kafatos, 1990; Tolias et al., 1993), no reported mutants disrupt DA-specific chorion expression.

The second function of *shark* lies in the stretch cells and affects the migration of the DA cells. Large stretch-cell clones resulted in shortened DAs that varied in their morphology and penetrance. This variability could result from residual activity of these mutant alleles (see Materials and methods), non-cell autonomy, or functional redundancy. Although no Shark paralogs are encoded in the genome (Adams et al., 2000), several non-receptor tyrosine kinases share homology in the SH2 and kinase domains, including Src42A.

In addition, stretch-cell expression of *shark* strongly suppressed the *bwk*-mutant DA phenotype, in concurrence with a direct role for *bwk* in regulating *shark* expression in this tissue. These results indicate that *shark* is key in regulating DA migration downstream of *bwk*. Full rescue was not likely achieved because of insufficient expression levels, the need to localize *shark* RNA, or the existence of *shark*-independent branches downstream of *bwk*.

These data suggest a model in which BWK regulates factors in the germline that are required for proper *shark* expression in the stretch cells. Shark then regulates the activity of targets required for DA-cell movement across the stretch-cell layer (Fig. 6A). Another factor that could be regulated by *bwk* is the *Src42A* kinase, which behaves similarly to *shark* (Fig. 6B). Loss of *Src42A* enhances *bwk* mutants, while stretch-cell expression of activated Src42A suppresses. Mammalian homologs of Shark function together with Src kinases, suggesting a conserved signaling cascade.

Stretch-cell signaling

Two other stretch-cell signaling pathways, JNK and DPP, regulate DA morphogenesis. Tests with *bwk* and *shark*, however, failed to reveal strong or definitive interactions. Loss of JNK activity in oogenesis results in shortened and paddleless DAs, yet expression of UAS-*basket*$^{+}$ and reduction of *bsk* dose did not alter the morphology of *bwk* eggshells. Furthermore, expression of the AP-1 components was unaffected in *bwk* mutants and *shark* clones. These data support the hypothesis that the *bwk*/*shark* pathway does not primarily act through JNK signaling.

Moderate overexpression of *dpp* and loss of the type I receptors, *tkv* and *sax*, can lead to shortened and somewhat broadened DAs, resembling *bwk* mutants (Twombly et al., 1996). The expression of *dpp* RNA and a *dpp* enhancer trap, however, were unaffected in *bwk* mutants. Both hypomorphic *dpp* alleles and loss of type I receptors failed to interact with

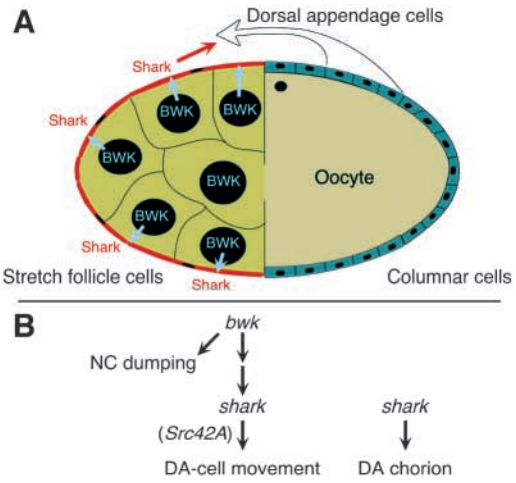

Fig. 6. Model of *bwk* and *shark* interactions. (A) Shark expression is regulated by BWK function in the germline. Shark activity in the stretch cells is required for the proper anterior movement of the DA-forming cells as they move anteriorly. (B) *bwk* and *shark* interactions. Shark in the stretch cells regulates DA-cell movement, while Shark in the DA-forming cells regulates synthesis of the DA chorion. The suppression of *bwk* by SRC42A stretch-cell expression suggests that this protein may function alongside Shark to mediate DA-cell movement.

a strong *bwk* mutant. Our data suggest that *bwk* does not directly regulate *dpp* expression or activity but rather may modulate downstream targets.

Stretch-cell function

DA-cell movement over the stretch cells may require expression of stretch-cell factors that guide or facilitate migration. As noted above, mammalian proteins that share homology with Shark can bind to and regulate integrin complexes. Shark may bind these and/or other adhesion receptors to regulate cell migration either through signaling cues or by modulating the extracellular matrix.

Shark could also regulate stretch cell behaviors, controlling the small cellular projections that extend towards the DA cells during their anterior movement. These extensions may guide or signal the DA-forming cells, as occurs in imaginal discs (Cho et al., 2000; Gibson and Schubiger, 2000; Ramirez-Weber and Kornberg, 1999).

Extracellular signals and interactions are key components of morphogenetic processes. We have identified two downstream components of the *bwk* pathway that act in the stretch-cell layer to relay a novel germline signal required for the movement of a third tissue, the remodeling epithelium of the dorsal appendage cells.

We thank R. Stanley, R. Warrior and P. Lasko for their generosity with the *shark* and *Bic-C* reagents. We thank M. Llimargas, S. Luschnig, S. Hou, M. Mlodzik, G. Boulianne, L. Manseau and H. Ruohola-Baker for reagents or equipment. We also thank the members of the Berg laboratory for helpful discussions.

References

Adams, M. D., Celniker, S. E., Holt, R. A., Evans, C. A., Gocayne, J. D., Amanatides, P. G., Scherer, S. E., Li, P. W., Hoskins, R. A., Galle, R. F. et al. (2000). The genome sequence of *Drosophila melanogaster*. *Science* **287**, 2185-2195.

Amrein, H. and Axel, R. (1997). Genes expressed in neurons of adult male *Drosophila*. *Cell* **88**, 459-469.

Bauer, B. J. and Waring, G. L. (1987). 7C female sterile mutants fail to accumulate early eggshell proteins necessary for later chorion morphogenesis in *Drosophila*. *Dev. Biol.* **121**, 349-358.

Bearz, A., Tell, G., Formisano, S., Merluzzi, S., Colombatti, A. and Pucillo, C. (1999). Adhesion to fibronectin promotes the activation of the p125(FAK)/Zap-70 complex in human T cells. *Immunology* **98**, 564-568.

Boutros, M., Paricio, N., Strutt, D. I. and Mlodzik, M. (1998). Dishevelled activates JNK and discriminates between JNK pathways in planar polarity and *wingless* signaling. *Cell* **94**, 109-118.

Brand, A. H. and Perrimon, N. (1993). Targeted gene expression as a means of altering cell fates and generating dominant phenotypes. *Development* **118**, 401-415.

Brand, A. H. and Perrimon, N. (1994). Raf acts downstream of the EGF receptor to determine dorsoventral polarity during *Drosophila* oogenesis. *Genes Dev.* **8**, 629-639.

Chan, A. C., Irving, B. A., Fraser, J. D. and Weiss, A. (1991). The zeta chain is associated with a tyrosine kinase and upon T-cell antigen receptor stimulation associates with ZAP-70, a 70-kDa tyrosine phosphoprotein. *Proc. Natl. Acad. Sci. USA* **88**, 9166-9170.

Chan, T. A., Chu, C. A., Rauen, K. A., Kroiher, M., Tatarewicz, S. M. and Steele, R. E. (1994). Identification of a gene encoding a novel protein-tyrosine kinase containing SH2 domains and ankyrin-like repeats. *Oncogene* **9**, 1253-1259.

Chen, H. W., Marinissen, M. J., Oh, S. W., Chen, X., Melnick, M., Perrimon, N., Gutkind, J. S. and Hou SX. (2002). CKA, a novel multidomain protein, regulates the JUN N-terminal kinase signal transduction pathway in *Drosophila*. *Mol. Cell Biol.* **22**,1792-1803.

Cho, K. O., Chern, J., Izaddoost, S. and Choi, K. W. (2000). Novel signaling from the peripodial membrane is essential for eye disc patterning in *Drosophila*. *Cell* **103**, 331-342.

Chou, T. B. and Perrimon, N. (1992). Use of a yeast site-specific recombinase to produce female germline chimeras in *Drosophila*. *Genetics* **131**, 643-653.

Chu, D. H., Morita, C. T. and Weiss, A. (1998). The Syk family of protein tyrosine kinases in T-cell activation and development. *Immunol. Rev.* **165**, 167-180.

Ciapponi, L., Jackson, D. B., Mlodzik, M. and Bohmann, D. (2001). Drosophila Fos mediates ERK and JNK signals via distinct phosphorylation sites. *Genes Dev.* **15**, 1540-1553.

Davis, I., Girdham, C. H. and O'Farrell, P. H. (1995). A nuclear GFP that marks nuclei in living *Drosophila* embryos; maternal supply overcomes a delay in the appearance of zygotic fluorescence. *Dev. Biol.* **170**, 726-729.

Dequier, E., Souid, S., Pal, M., Maroy, P., Lepesant, J. A. and Yanicostas, C. (2001). Top-DER- and Dpp-dependent requirements for the *Drosophila fos/kayak* gene in follicular epithelium morphogenesis. *Mech. Dev.* **106**, 47-60.

Dobens, L. L., Martin-Blanco, E., Martinez-Arias, A., Kafatos, F. C. and Raftery, L. A. (2001). *Drosophila puckered* regulates Fos/Jun levels during follicle cell morphogenesis. *Development* **128**, 1845-1856.

Dorman, J. B., James, K. E., Fraser, S. E., Kiehart, D. P. and Berg, C. A. (2004). *bullwinkle* is required for epithelial morphogenesis during *Drosophila* oogenesis. *Dev. Biol.* (in press).

Fernandez, R., Takahashi, F., Liu, Z., Steward, R., Stein, D. and Stanley, E. R. (2000). The *Drosophila* Shark tyrosine kinase is required for embryonic dorsal closure. *Genes Dev.* **14**, 604-614.

Ferrante, A. W., Jr, Reinke, R. and Stanley, E. R. (1995). Shark, a Src homology 2, ankyrin repeat, tyrosine kinase, is expressed on the apical surfaces of ectodermal epithelia. *Proc. Natl. Acad. Sci. USA* **92**, 1911-1915.

French, R. L., Cosand, K. A. and Berg, C. A. (2003). The Drosophila female sterile mutation *twin peaks* is a novel allele of *tramtrack* and reveals a requirement for Ttk69 in epithelial morphogenesis. *Dev. Biol.* **253**, 18-35.

Fristrom, D. F. J. (1993). The metamorphic development of the adult epidermis. In *The Development of* Drosophila melanogaster, Vol. 2 (ed. M. Bate and A. Martinez Arias), pp. 843-898. New York: Cold Spring Harbor Laboratory Press.

Gibson, M. C. and Schubiger, G. (2000). Peripodial cells regulate proliferation and patterning of *Drosophila* imaginal discs. *Cell* **103**, 343-350.

Golic, K. G. and Lindquist, S. (1989). The FLP recombinase of yeast catalyzes site-specific recombination in the *Drosophila* genome. *Cell* **59**, 499-509.

Gustafson, K. and Boulianne, G. L. (1996). Distinct expression patterns detected within individual tissues by the GAL4 enhancer trap technique. *Genome* **39**, 174-182.

Harden, N., Ricos, M., Yee, K., Sanny, J., Langmann, C., Yu, H., Chia, W. and Lim, L. (2002). Drac1 and Crumbs participate in amnioserosa morphogenesis during dorsal closure in *Drosophila*. *J. Cell Sci.* **115**, 2119-2129.

Jacinto, A., Woolner, S. and Martin, P. (2002). Dynamic analysis of dorsal closure in *Drosophila*: from genetics to cell biology. *Dev. Cell* **3**, 9-19.

Kiehart, D. P., Galbraith, C. G., Edwards, K. A., Rickoll, W. L. and Montague, R. A. (2000). Multiple forces contribute to cell sheet morphogenesis for dorsal closure in *Drosophila*. *J. Cell Biol.* **149**, 471-490.

King, R. C. and Koch, E. A. (1963). Studies on ovarian follicle cells of Drosophila. *Quart. J. Micro. Sci.* **104**, 293-320.

Knust, E. (1997). *Drosophila* morphogenesis: movements behind the edge. *Curr. Biol.* **7**, R558-561.

Lamka, M. L. and Lipshitz, H. D. (1999). Role of the amnioserosa in germ band retraction of the *Drosophila melanogaster* embryo. *Dev. Biol.* **214**, 102-112.

Landis, G., Kelley, R., Spradling, A. C. and Tower, J. (1997). The *k43* gene, required for chorion gene amplification and diploid cell chromosome replication, encodes the *Drosophila* homolog of yeast origin recognition complex subunit 2. *Proc. Natl. Acad. Sci. USA* **94**, 3888-3892.

Latour, S. and Veillette, A. (2001). Proximal protein tyrosine kinases in immunoreceptor signaling. *Curr. Opin. Immunol.* **13**, 299-306.

Lee, T., Winter, C., Marticke, S. S., Lee, A. and Luo, L. (2000). Essential roles of *Drosophila* RhoA in the regulation of neuroblast proliferation and dendritic but not axonal morphogenesis. *Neuron* **25**, 307-316.

Mahajan-Miklos, S. and Cooley, L. (1994). Intercellular cytoplasm transport during *Drosophila* oogenesis. *Dev. Biol.* **165**, 336-351.

Mahone, M., Saffman, E. E. and Lasko, P. F. (1995). Localized *Bicaudal-C* RNA encodes a protein containing a KH domain, the RNA binding motif of FMR1. *EMBO J.* **14**, 2043-2055.

Manseau, L., Baradaran, A., Brower, D., Budhu, A., Elefant, F., Phan, H., Philp, A. V., Yang, M., Glover, D., Kaiser, K. et al. (1997). GAL4 enhancer traps expressed in the embryo, larval brain, imaginal discs, and ovary of *Drosophila*. *Dev. Dyn.* **209**, 310-322.

Margaritis, L. H., Kafatos, F. C. and Petri, W. H. (1980). The eggshell of *Drosophila melanogaster*. I. Fine structure of the layers and regions of the wild-type eggshell. *J. Cell Sci.* **43**, 1-35.

Margolis, J. and Spradling, A. (1995). Identification and behavior of epithelial stem cells in the *Drosophila* ovary. *Development* **121**, 3797-3807.

Mohler, D. and Carroll, A. (1984). Report of new mutants. *Dros. Inf. Serv.* **60**, 236-241.

Nilson, L. A. and Schüpbach, T. (1998). Localized requirements for *windbeutel* and *pipe* reveal a dorsoventral prepattern within the follicular epithelium of the *Drosophila* ovary. *Cell* **93**, 253-262.

Peri, F. and Roth, S. (2000). Combined activities of Gurken and Decapentaplegic specify dorsal chorion structures of the *Drosophila* egg. *Development* **127**, 841-850.

Queenan, A. M., Ghabrial, A. and Schüpbach, T. (1997). Ectopic activation of *torpedo/Egfr*, a *Drosophila* receptor tyrosine kinase, dorsalizes both the eggshell and the embryo. *Development* **124**, 3871-3880.

Ramirez-Weber, F. A. and Kornberg, T. B. (1999). Cytonemes: cellular processes that project to the principal signaling center in *Drosophila* imaginal discs. *Cell* **97**, 599-607.

Reed, B. H., Wilk, R. and Lipshitz, H. D. (2001). Downregulation of Jun kinase signaling in the amnioserosa is essential for dorsal closure of the *Drosophila* embryo. *Curr. Biol.* **11**, 1098-1108.

Riese, J., Tremml, G. and Bienz, M. (1997). D-Fos, a target gene of Decapentaplegic signalling with a critical role during *Drosophila* endoderm induction. *Development* **124**, 3353-3361.

Riesgo-Escovar, J. R., Jenni, M., Fritz, A. and Hafen, E. (1996). The *Drosophila* Jun-N-terminal kinase is required for cell morphogenesis but not for DJun-dependent cell fate specification in the eye. *Genes Dev.* **10**, 2759-2768.

Rittenhouse, K. R. and Berg, C. A. (1995). Mutations in the *Drosophila* gene *bullwinkle* cause the formation of abnormal eggshell structures and bicaudal embryos. *Development* **121**, 3023-3033.

Schock, F. and Perrimon, N. (2002). Cellular processes associated with germ band retraction in *Drosophila*. *Dev. Biol.* **248**, 29-39.

Schüpbach, T. (1987). Germ line and soma cooperate during oogenesis to establish the dorsoventral pattern of egg shell and embryo in *Drosophila melanogaster*. *Cell* **49**, 699-707.

Schüpbach, T. and Wieschaus, E. (1991). Female sterile mutations on the second chromosome of *Drosophila melanogaster*. II. Mutations blocking oogenesis or altering egg morphology. *Genetics* **129**, 1119-1136.

Soede, R. D., Wijnands, Y. M., van Kouteren-Cobzaru, I. and Roos, E. (1998). ZAP-70 tyrosine kinase is required for LFA-1-dependent T cell migration. *J. Cell Biol.* **142**, 1371-1379.

Spradling, A. (1993). Developmental genetics of oogenesis. In *The Development of* Drosophila melanogaster (ed. M. Bate and A. Martinez-Arias), pp. 1-69. Cold Spring Harbor: Cold Spring Harbor Laboratory Press.

Stronach, B. E. and Perrimon, N. (2001). Investigation of leading edge formation at the interface of amnioserosa and dorsal ectoderm in the *Drosophila* embryo. *Development* **128**, 2905-2913.

Suga, H., Koyanagi, M., Hoshiyama, D., Ono, K., Iwabe, N., Kuma, K. and Miyata, T. (1999). Extensive gene duplication in the early evolution of animals before the parazoan-eumetazoan split demonstrated by G proteins and protein tyrosine kinases from sponge and hydra. *J. Mol. Evol.* **48**, 646-653.

Suzanne, M., Perrimon, N. and Noselli, S. (2001). The *Drosophila* JNK pathway controls the morphogenesis of the egg dorsal appendages and micropyle. *Dev. Biol.* **237**, 282-294.

Taniguchi, T., Kobayashi, T., Kondo, J., Takahashi, K., Nakamura, H., Suzuki, J., Nagai, K., Yamada, T., Nakamura, S. and Yamamura, H. (1991). Molecular cloning of a porcine gene *syk* that encodes a 72-kDa protein-tyrosine kinase showing high susceptibility to proteolysis. *J. Biol. Chem.* **266**, 15790-15796.

Tateno, M., Nishida, Y. and Adachi-Yamada, T. (2000). Regulation of JNK by Src during *Drosophila* development. *Science* **287**, 324-327.

Tautz, D. and Pfeifle, C. (1989). A non-radioactive in situ hybridization method for the localization of specific RNAs in *Drosophila* embryos reveals translational control of the segmentation gene hunchback. *Chromosoma* **98**, 81-85.

Tolias, P. P. and Kafatos, F. C. (1990). Functional dissection of an early *Drosophila* chorion gene promoter: expression throughout the follicular epithelium is under spatially composite regulation. *EMBO J.* **9**, 1457-1464.

Tolias, P. P., Konsolaki, M., Halfon, M. S., Stroumbakis, N. D. and Kafatos, F. C. (1993). Elements controlling follicular expression of the s36 chorion gene during *Drosophila* oogenesis. *Mol. Cell. Biol.* **13**, 5898-5906.

Twombly, V., Blackman, R. K., Jin, H., Graff, J. M., Padgett, R. W. and Gelbart, W. M. (1996). The TGF- signaling pathway is essential for *Drosophila* oogenesis. *Development* **122**, 1555-1565.

Waring, G. L. (2000). Morphogenesis of the eggshell in *Drosophila*. *Int. Rev. Cytol.* **198**, 67-108.

Wasserman, J. D. and Freeman, M. (1998). An autoregulatory cascade of EGF receptor signaling patterns the *Drosophila* egg. *Cell* **95**, 355-364.

Xu, T. and Rubin, G. M. (1993). Analysis of genetic mosaics in developing and adult *Drosophila* tissues. *Development* **117**, 1223-1237.